5th International Symposium on Hydraulic Structures Brisbane, Australia, 25-27 June 2014
Hydraulic Structures and Society: Engineering Challenges and Extremes
ISBN 9781742721156 - DOI: 10.14264/uql.2014.29

Air concentration distribution in deflector-jets

M. Pfister and S. Schwindt
Laboratoire de Constructions Hydrauliques (LCH)
Ecole Polytechnique Fédérale de Lausanne (EPFL)
CH – 1015 Lausanne
SWITZERLAND
E-mail: michael.pfister@epfl.ch

Abstract: *As an alternative to ski jumps, deflectors can be implemented on spillways to generate free jets. They guide, up to a certain limit, the jet to an achieved location onto the plunge pool surface, and furthermore enhance the process of jet disintegration. The present research addresses the following aspects, derived from physical model tests: (1) length and shape of the jet black-water core and further characteristic air concentration contour lines, (2) streamwise development of average and minimum sectional air concentrations, as well as jet thickness, and (3) sectional air concentration profiles along the jet. It is shown that all mentioned parameters depend only on the relative black-water core length, being a function of the approach flow characteristics, the deflector geometry and the chute slope.*

Keywords: *Air concentration, Black-water core, Deflector, Jet.*

1. INTRODUCTION

Free jets are frequently generated by hydraulic structures. Examples are drop manholes in sewer systems, or on spillways at dams. Particularly on spillways, some jet features are provoked intentionally by providing a specific jet take-off structure at the chute end, as for instance a ski jump or a deflector. These devices enhance the flow turbulence and support thus the disintegration process of the jet, and furthermore guide the jet to a certain impact location on the plunge pool water surface.

On spillways, ski jumps are a standard dissipation element. Recently, an alternative concept for jet generation was presented by Steiner et al. (2008), namely the triangular deflector. The main advantage of such deflectors is their reduced constructional cost because of simple form work, particularly if providing a 3D terminal structure with a transverse variable geometry for horizontal jet deflection. A disadvantage might be that the application range of deflectors is presumably limited to relatively flat chutes and to bottom outlets. An efficient flow deflection providing a jet impact location far away from the take-off structure is impossible downstream of steep chutes, because the total deviation angle for deflectors is smaller than for ski jumps. A hydraulic comparison of flip bucket and deflector generated jets indicate that: (1) The local maximum dynamic pressure on deflectors is larger than on the corresponding flip buckets, whereas the total dynamic pressure force is smaller; (2) A deflector results in longer throwing distances than a flip bucket for identical boundary conditions; (3) The jet energy dissipation characteristics of both designs is comparable; and (4) No significant differences were found in the flow choking features.

Hydraulics of deflector-generated jets was investigated by Steiner et al. (2008), as well as by Pfister and Hager (2009). The first publication focuses on the jet trajectories, whereas the second provides information regarding the minimum and average air concentration characteristics along such jets. Particularly, it was shown that these air features depend uniquely on the relative jet black-water core length, defined between the jet take-off and the jet profile with a minimum air concentration of $C_m = 0.01$. The present paper re-evaluates these data including additional tests conducted with exceptionally steep deflectors (Pfister 2011), generating particularly long and aerated jets, so that the previous result could be extended. Furthermore, general air concentration profiles, again as a function of the relative jet black-water core length, are presented. These appear similar to those recorded by Toombes and Chanson (2007) for bottom outlet jets without deflector.

The main parameters used to describe the air concentration distribution within a deflector-generated jet take into account the geometrical and hydraulic features at the take-off, namely (Fig. 1) the

approach flow depth h_o, the approach flow velocity V_o, the approach flow Froude number $F_o = V_o/(gh_o)^{0.5}$, the chute bottom angle φ, the deflector height t (perpendicular to the chute bottom), and the deflector angle α. All these parameters were systematically varied in the frame of a physical model investigation. The basic data of the study of Pfister and Hager (2009) were used, after filtering them. Exclusively tests with (1) atmospheric pressure below the jet, (2) not pre-aerated approach flow, and (3) a black-water core shorter than the jet were considered. Furthermore, no drop-generated jets (absence of a deflector) were taken into account. Finally, 58 tests remained, all including some 3 to 10 air concentration profiles along the jet. As indicated in Fig. 1, the streamwise coordinate x starts at the deflector take-off lip and is parallel to the chute bottom, and the coordinate z is orientated perpendicular to x. The limits of the study, as a result of the test conditions in the physical model, are $0.047 \text{ m} \le h_o \le 0.086 \text{ m}$, $5.9 \le F_o \le 10.4$, $5.7° \le \alpha \le 26.6°$, and $12° \le \varphi \le 50°$. Scale effects concerning air concentrations are presumably small, because the recommendations of Pfister and Chanson (2012) are respected. Namely, the approach flow Weber number $W_o = (\rho V_o^2 h_o)/\sigma$ ranged between $143 \le W_o^{0.5} \le 234$, and the approach flow Reynolds number $R_o = V_o h_o/\nu$ ranged between $2.6\ 10^5 \le R_o \le 5.2\ 10^5$. Note that ρ = water density, σ = water surface tension, and ν = water kinematic viscosity.

Air concentration $C(z, x)$ profiles were section-wise measured, using a double-tip fibre-optical probe. The streamwise spacing between the individual profiles was constant as Δx=0.200 m, and the spacing along the z coordinate was about 0.002 to 0.005 m. The upper (subscript U) and the lower (subscript L) jet trajectories $z_U(x)$ and $z_L(x)$ were defined along the jet boundaries similar to C = 0.90.

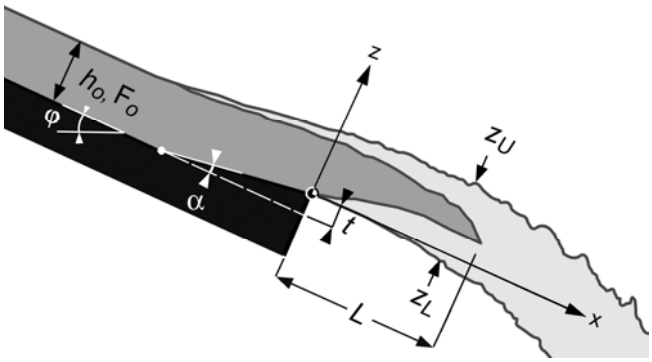

Figure 1 – Definition sketch for deflector-generated jets (Pfister and Hager 2009)

2. BLACK-WATER CORE

2.1. Standard definition

The break-up length of a jet is typically linked to the length of its coherent black-water core. Deriving such a black-water core from the present data requires (1) that the approach flow consists mainly of black-water (tests with artificially pre-aerated approach flow were excluded), and (2) a criterion to define “black-water”, herein chosen as $C \le 0.01$. Accordingly, the present black-water core ranges between the jet take-off at x=0.0 m, and the profile at a certain streamwise location x where the sectional minimum (subscript m) air concentration is C_m = 0.01. Then, jet parts upstream of the latter location include $C_m < 0.01$, and parts downstream include $C_m > 0.01$. Because the criterion of C_m = 0.01 was never precisely within a measured profile, a linear interpolation between the two neighbouring profiles was conducted.

The black-water core length L_1 (Fig. 1) as derived from the model tests and using the C = 0.01 criterion was normalized with h_o. The main parameters affecting L/h_o were identified as F_o, α and φ, so that (Pfister and Hager 2009)

$$\frac{L_1}{h_o} = 73 \mathrm{F}_o^{-1} \left(1 + tan\alpha\right)^{-0.5} \left(1 + sin\varphi\right) \quad (1)$$

The coefficient of determination between measured values and those derived from Eq. (1) is R^2 = 0.87. Given that Eq. (1) bases on the C = 0.01 criterion (1% of air concentration), the related black-water core length is denoted as L_1.

2.2. Extended definition

The criterion to define the black-water core length (C_m = 0.01) might be modified to C_m =0.05 or C_m = 0.10, for instance. Of course, one may then not consider the resulting lengths as a "black-water core" any more, but rather as characteristic jet disintegration lengths. Given that the latter correlate with the normalization as prosed in Eq. (1), they are indicated herein anyway. The two new definitions include thus lengths reaching between take-off and the sectional profile with a minimum air concentration of either C_m = 0.05 or C_m = 0.10. The related lengths are denoted as L_5 (up to 5% air concentration) and L_{10} (up to 10%). The individual lengths all depend on the normalization of Eq. (1), but with different inclinations of the linear best fit. Note that the subscript i stands for the different criteria, i.e. 1%, 5% and 10%. Then

$$\frac{L_i}{h_o} = B_i \, \mathrm{F}_o^{-1} \left(1 + tan\alpha\right)^{-0.5} \left(1 + sin\varphi\right) \quad (2)$$

with B_1 = 73 for L_1 (i = 1%, i.e. similar to Eq. (1)), B_5 = 105 for L_5 (i = 5%), and B_{10} = 130 for L_{10} (i = 10) (Table 1). The coefficients of determination between measured values and those derived from Eq. (2) are R^2 = 0.86 for L_5, and R^2 = 0.82 for L_{10}. The individual values L_i/h_o derived from the model data are shown versus the normalized abscissa being

$$\Phi = \mathrm{F}_o^{-1} \left(1 + tan\alpha\right)^{-0.5} \left(1 + sin\varphi\right) \quad (3)$$

in Fig. 2a. Dividing the B_5 and B_{10} values by the black-water core factor B_1 results in B_5/B_1 = 105/73 = 1.44 (close to √2), and B_{10}/B_1 = 130/73 = 1.78 (close to √3). In average, a minimum sectional air concentration of C_m = 0.05 was observed at 1.44 times the black-water core length, and a C_m = 0.10 at 1.78 times the black-water core length. If considering the individually measured L_5/L_1 and L_{10}/L_1 per particular jet results in similar values, as shown in the histogram of Fig. 2b. From these individual factors per jet, an average of L_5/L_1 = 1.46 and of L_{10}/L_1 = 1.81 followed. This is close to the global ratios derived from the B_i as indicated before.

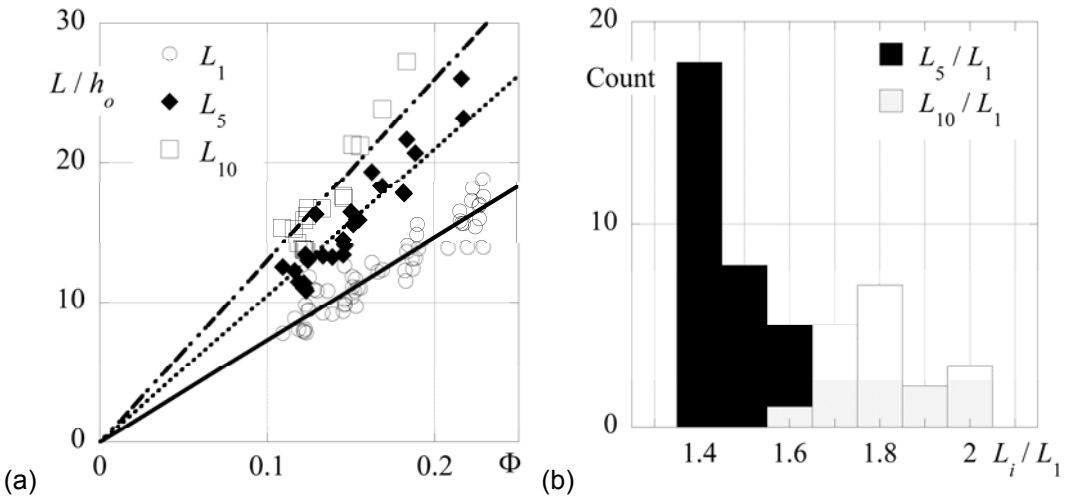

Figure 2 – Normalized lengths, (a) for cores reaching up to C_m = 0.01 (L_1, black-water), C_m = 0.05 (L_5), and C_m = 0.10 (L_{10}), all as a function of Φ according to Eq. (3), and (b) histogram showing distribution of individual L_{10}/L_1 and L_5/L_1

2.3. Shape

The black-water core shape (contour lines defined at C = 0.01, visible as coherent black-water in Fig. 3) as well as the contour lines at C = 0.05 and C = 0.10 were derived from the model data. They are shown in Fig. 4, with a normalized ordinate as

$$Z = \frac{z - z_L}{z_U - z_L} \tag{4}$$

At every section, the location Z = 1 correspond accordingly to the upper jet trajectory (at C = 0.90) and Z = 0 to the lower jet trajectory. The abscissa is given as

$$\chi = \frac{x}{L_1} \tag{5}$$

denoted as relative black-water core length. Consequently, the black-water core with C < 0.01 spans between X = 0 and X = 1. Depending on the chosen criterion from chapter 2.2, the characteristic jet lengths L_5/L_1 = 1.44 and L_{10}/L_1 = 1.78 correspond to X = 1.44 and X = 1.78, respectively (Fig. 4). Both, the upper and the lower contour lines derived for each criterion may be approximated with similar square-root-functions as

$$Z_U = 1 - D\sqrt{\chi} \tag{6}$$

$$Z_L = E\sqrt{\chi} \tag{7}$$

The parameters D and E are given in Table 1, in function of the different criteria. Figure 4 shows the jet black-water core shape (Fig. 4a), and the two related characteristic contour lines (Fig. 4b, c) normalized with Eqs. (4) and (5). The data and the trend lines according to Eqs. (6) and (7) essentially collapse. The relative elevation of the black-water core end within the jet – and also the elevation where the normalized contour lines of the two supplementary criteria merge – is at about 0.7Z. These observations agree with the visual impression of the black-water core shape as shown in Fig. 3.

Table 1 – Parameters to derive air characteristics for various criteria

Criteria C [-]	Subscript i	B [-] Eq. (2)	D [-] Eq. (6)	E [-] Eq. (7)
0.01	1	73	0.29	0.71
0.05	5	105	0.23	0.60
0.10	10	130	0.21	0.53

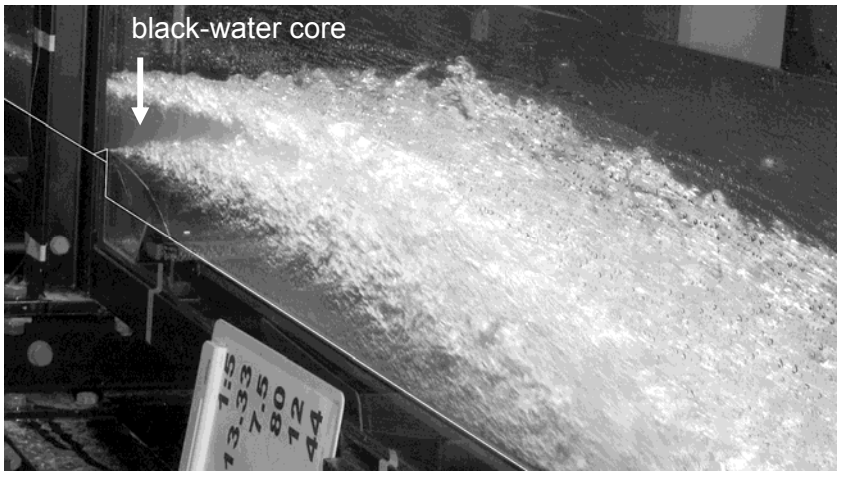

Figure 3 – Photo of deflector-generated jet with black-water core for h_o = 0.080 m, F_o = 7.5, φ = 12°, t = 0.013 m, and α = 11.3°

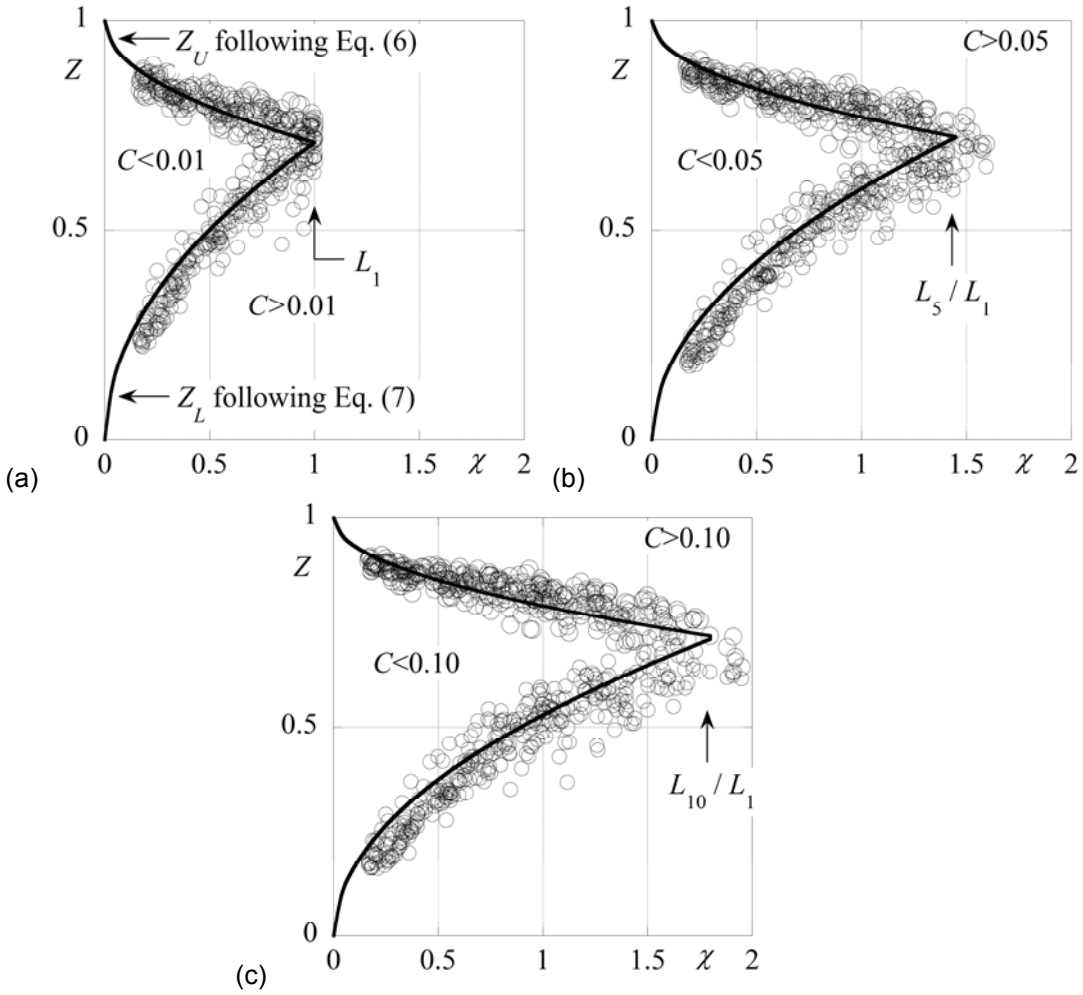

Figure 4 – Contour lines $Z(X)$, for (a) black-water core defined along the contour-line C = 0.01, (b) along the contour line C = 0.05, and (c) along the contour line C = 0.10

3. STREAMWISE CHARACTERISTIC PARAMETERS

The description of the contour lines of the jet black-water core and those in its vicinity (Fig. 4) reveals the importance of the streamwise normalization X. As reported by Pfister and Hager (2009), the parameter X determines the complete jet air concentration distribution. Consequently, characteristic values linked to the latter can be derived. Such a characteristic value is the average (subscript a) air concentration per jet section. The latter results from an integration of $C(z)$ and a division by the jet thickness $h_j = z_U - z_L$, resulting in (Straub and Anderson 1958)

$$C_a = \frac{1}{h_j}\int_{z_L}^{z_U} C(z)\,\mathrm{d}z \tag{8}$$

The data indicate that the streamwise development of C_a along the jet is

$$C_a = tanh\left(0.4\sqrt{\chi}\right) \tag{9}$$

Figure 5a shows the values derived from the tests and Eq. (9). The coefficient of determination is R^2 = 0.93, furthermore Eq. (9) is valid between $0 \le X \le 6$. The streamwise sectional minimum (subscript m) air concentration also depends on X, and is expressed as

$$C_m = 0.6\,tanh\left[\left(\sqrt{\chi}-1\right)^2\right] + 0.01 \tag{10}$$

The determination of Eq. (10) and the data is R^2 = 0.93, the range of validity includes $1 \le X \le 6$, and the data and Eq. (10) are compared in Fig. 5b. The relative elevation of C_m within a jet section is denoted as Z_m, i.e. normalized according to Eq. (4) inserting $z = z_m$. As visible in Fig. 5c, Z_m is typically located between $0.6 \le Z \le 0.8$ along roughly $0.5 < X < 2$, i.e. on a relatively high elevation within the jet. This is probably due to the flow turbulence initiated at the chute bottom along the approach flow part, particularly acting on the lower jet surface disintegration. Note that no points were derived in the range $X \le 0.5$, because $C_m \approx 0$ covers a considerable relative jet height (see Fig. 6a, typically more than $0.5 < Z < 0.8$), not allowing to determine *one* Z_m. Along $X > 3$ one may observe $Z_m \rightarrow 0.5$ to 0.6, approaching a symmetrical jet characteristic far away from take-off.

The relative jet thickness h_j increases with jet length, as the jet disperses. The data indicate a linear dispersion along X as

$$\frac{h_j}{h_o} = 1.1 + 0.35\chi \tag{11}$$

The initial relative jet thickness at the take-off ($X = 0$) is around $h_j/h_o = 1.1$, and thus 10% larger than h_o. This is a consequence of the rough flow surface initiated at the beginning of the deflector (see Fig. 3). Here, R^2 = 0.81, the limits of Eq. (11) are again $0 \le X \le 6$, and a comparison of the data and Eq. (11) is given in Fig. 5d.

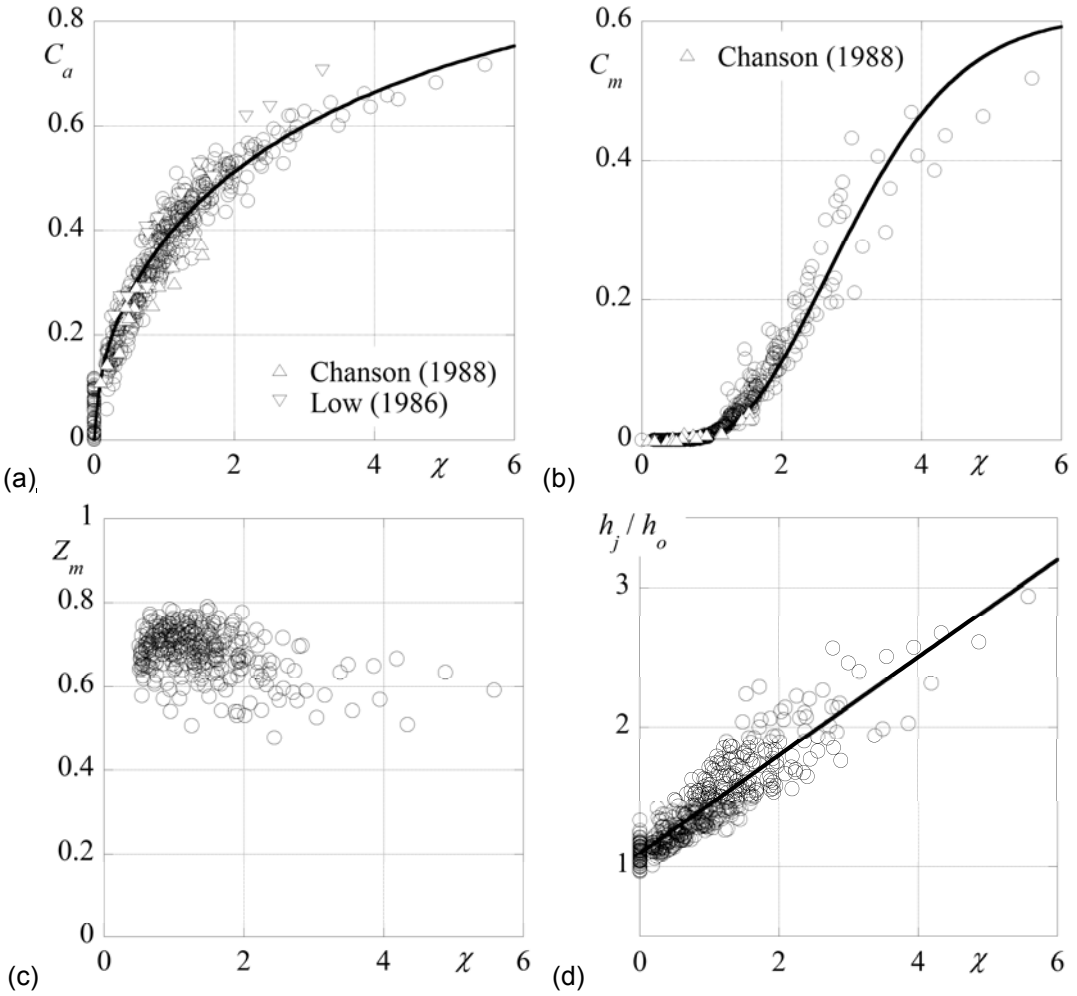

Figure 5 – Jet air features versus relative black-water core length X, (a) C_a with (–) Eq. (9), (b) C_m with (–) Eq. (10), (c) Z_m, and (d) h_j/h_o with (–) Eq. (11)

4. AIR CONCENTRATION PROFILES

The sectional air concentration profiles also depend on X, similar to the streamwise characteristic parameters discussed before. The profiles are shown in Fig. (6) at various X (±10%), with a normalized jet thickness following Eq. (4). It is visible that the data collapse, independent of the take-off conditions. As shown in Figs. 4 and 5b, the profiles are asymmetrically at small X, indicating higher concentrations near the lower trajectory. Then, at $X > 3$, the air concentration profiles become almost symmetrically with Z_m at 0.5 to 0.6. Furthermore, the increase of C_m with X (Fig. 5b) is recognisable.

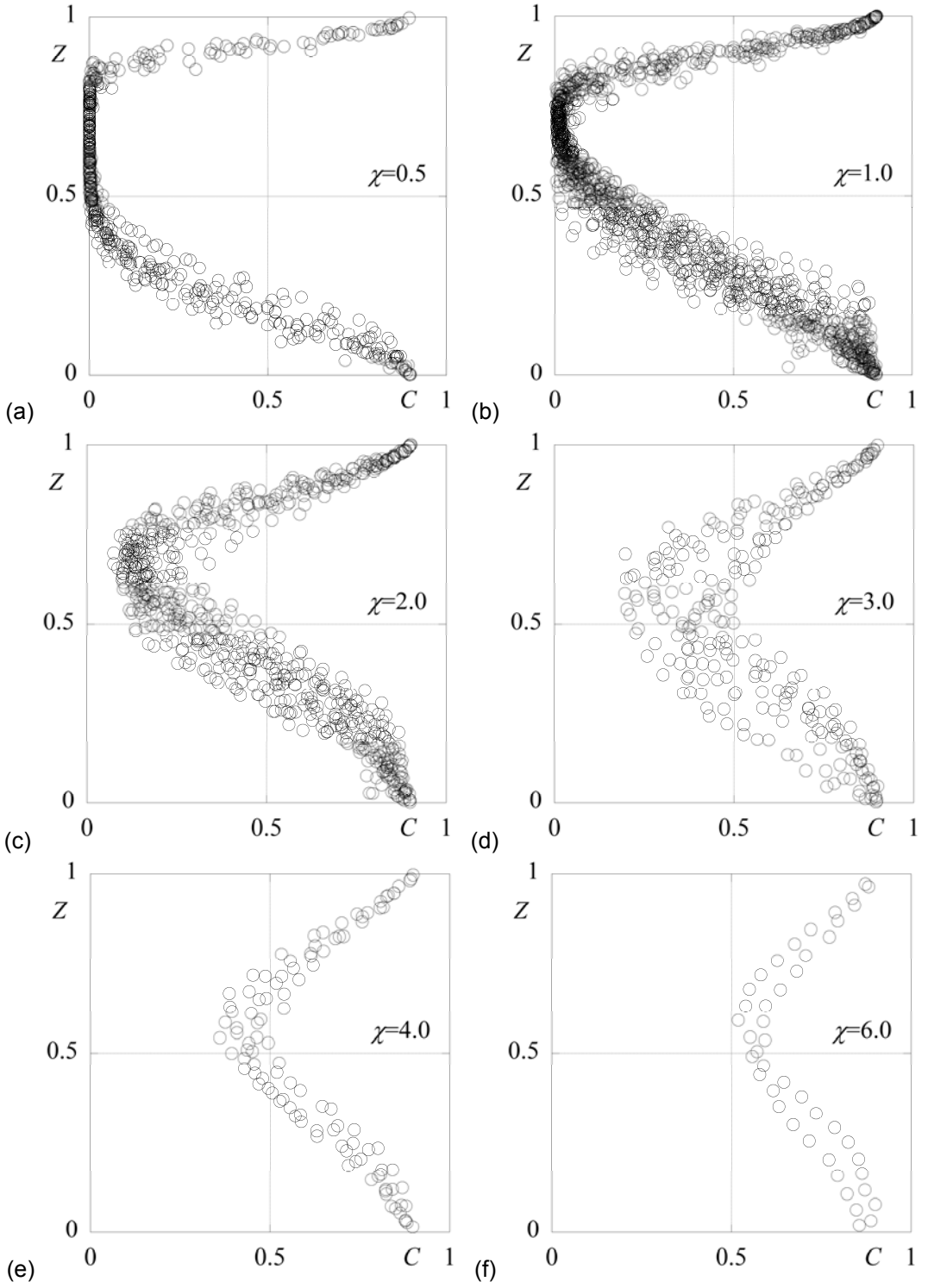

Figure 6 – Normalized jet air concentration profiles $C(Z)$ at different X (±10%), namely X = (a) 0.5, (b) 1.0, (c) 2.0, (d) 3.0, (e) 4.0, and (f) 6.0

5. CONCLUSIONS

The air concentration characteristics along a defector-generated jet are linked to its relative black-water core length. This characteristic length describes the non-aerated (i.e. with air concentrations below 1%) inner jet extension and determines the development of the average and minimum air concentrations along the jet. The normalized jet thickness also depends on the relative black-water core length, linked manly to the growth of the average air concentration. Given the latter observations, it is possible to demonstrate the dependence of the general sectional air concentration profile on the relative black-water core length. The jet black-water core length is mainly influenced by the approach flow depth and Froude number, the equivalent deflector angle, and the chute bottom angle.

The jet core consisting of black-water ($C \leq 0.01$) is asymmetrically and non-linear. The lower jet face disintegrates and aerates faster than the upper, as a result of the friction-induced turbulence originating from the chute bottom and the deflector. Contour lines considering higher air concentrations ($C = 0.05$ and 0.10) follow a similar but extended trend. Sectional air concentration profiles collapse when illustrated for a certain relative black-water core length, independent of the hydraulic and geometrical conditions under which the jet was generated. As a consequence, the average and minimum sectional concentrations for a given relative black-water core length may be derived as a function of the latter.

The average air concentration is $C_a = 0.38$ at the end of the black-water core (i.e. at L_1). Further downstream, the value still increases, but with a much reduced growth rate. This indicates that the disintegration process principally occurs close after take-off, where the turbulence initiated by the latter is mostly operative. Far away from take-off, the average concentration tends asymptotically towards 0.8 or even higher values. Typically, the minimum streamwise air concentration is not located at the jet centre, but above the latter as mentioned before. It tends, however, towards the jet centre for long jets. Finally, the jet thickness also increases with jet length, again in function of the relative black-water-core length. The trend was approximated with a simple linear function up to a relative jet length equivalent to six times the black-water core, although rather long jets tend to a finite thickness.

For hydraulic engineering, the herein presented results might be of interest to estimate jet air concentration features. These give, for instance, an indication of the air demand in drop manholes of sewer systems, or characterise on spillways the jet features at impact onto a plunge pool. These are, among other parameters, required to describe the scouring potential of jets (Pagliara et al. 2006, Bollaert and Schleiss 2003).

6. REFERENCES

Bollaert, E.F.R., Schleiss, A.J. (2003). *Scour of rock due to the impact of plunging high velocity jets 1: A state-of-the-art review*. Journal of Hydraulic Research 41(5), 451-464.

Chanson, H. (1988). *A study of air entrainment and aeration devices on a spillway model*. PhD Thesis, Dept. of Civ. Engng., Univ. of Canterbury, Christchurch, NZ.

Low, H.S. (1986). *Model studies of Clyde dam spillway aerators*. Research Report 86-6, Dept. of Civ. Engng., Univ. of Canterbury, Christchurch, NZ

Pagliara, S., Hager, W.H., Minor, H.-E. (2006). *Hydraulics of plane plunge pool scour*. Journal of Hydraulic Engineering 132(5), 450–461.

Pfister, M. (2011). *Chute aerators: Steep deflectors and cavity sub-pressure*. Journal of Hydraulic Engineering 137(10), 1208-1215.

Pfister, M., Chanson, H. (2012). *Discussion of scale effects in physical hydraulic engineering models*. Journal of Hydraulic Research 50(2), 244-246.

Pfister, M., Hager, W.H. (2009). *Deflector-generated jets*. Journal of Hydraulic Research 47(4), 466-475.

Straub, L.G., Anderson, A.G. (1958). *Experiments on self-aerated flow in open channels*. J. Hydraulics Div. 84(7), 1-35.

Steiner, R., Heller, V., Hager, W.H., Minor, H.-E. (2008). *Deflector ski jump hydraulics*. Journal of Hydraulic Engineering 134(5), 562-571.

Toombes, L., Chanson, H. (2007). *Free-surface aeration and momentum exchange at a bottom outlet*. Journal of Hydraulic Research 45(1), 100-110.